ECCOMAS Congress 2016
VII European Congress on Computational Methods in Applied Sciences and Engineering
M. Papadrakakis, V. Papadopoulos, G. Stefanou, V. Plevris (eds.)
Crete Island, Greece, 5–10 June 2016

EXTENSION AND APPLICATION OF A NONLINEAR REDUCED ORDER MODEL TO GUST LOAD PREDICTION IN TIME DOMAIN

C. Strobach[1], **K. Lindhorst**[1], **M. C. Haupt**[1], **P. Horst**[1]

[1] TU Braunschweig, Institute of Aircraft Design and Leightweight Structures
Hermann-Blenk-Str. 35
38108 Braunschweig
e-mail: {c.strobach, k.lindhorst, m.haupt, p.horst}@tu-bs.de

Keywords: reduced order models, gust load prediction, disturbance velocity approach

Abstract. *This paper aims at extending a markov chain based reduced order model to discrete gust load prediction in an aeroelastic simulation. An method for the incorporation of the disturbance velocity approach is presented and evaluated for the AGARD445 wing based on different training strategies. The reduced order model trained under elastic and gust load conditions can successfully predict the gust response in a rigid and in an elastic setup. Thus the presented ROM approach can serve as one single CFD surrogate model to predict aerodynamic forces under multiple loading conditions.*

1 Introduction

Efficient gust response analysis is crutial in aircraft design. Compared to linear aerodynamic models, URANS-solver can capture nonlinear effects in the transonic flow regime such as separation and shock movement at the cost of high computing times. Reduced order models (ROM) can reduce this computational cost significantly which is very important for coupled fluid-structure interaction simulations of large aircraft structures [16, 9].

ROMs for gust load caluations have been established using a linear aerodynamic model [4] or by a correction of doublet-lattice results [2]. [17] applied a disturbance velocities approach(DVA) in a linear aerodynamic state space formulation for the construction of a ROM that is capable of predicting generalized aerodynamic coefficients.

Recently [8] presented a reduced order model, that combines proper orthogonal decomposition (POD) and a discrete Markov chain with nonlinear mapping functions for the prediction of aerodynamic loads in the time domain. This paper presents an approach for the direct incorporation of the DVA [6] into this markov chain based ROM and an application to the 3D AGARD445.6 benchmark configuration under a discrete gust.

Using a predefined displacement sweep function to superimpose the first structural eigenmodes the ROM is trained with the computed nonlinear aerodynamic response of a forced motion analysis in TAU. Limit cycle oscillations (LCO) can be sufficiently predicted even for complex 3D configurations in the transsonic flow regime [9]. Extending the ansatz for the input displacements of the ROM with the discrete disturbance velocities, gust loads can be predicted.

AGARD model The well known benchmark case of the AGARD445 wing, experimentally studied by Yates [15], is choosen as a 3D example of the presented methods. The aerodynamic and structural model are depicted in Fig. 1. The corresponding structural eigenmodes are shown in Fig. 2 and listed in Table 1.

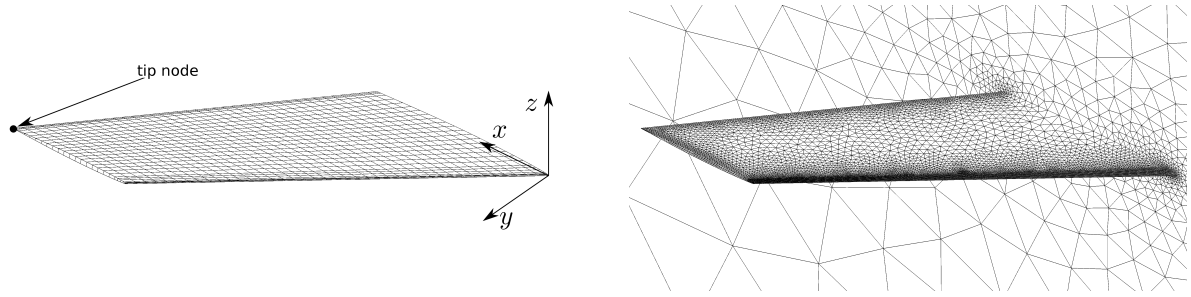

(a) (b)

Figure 1: AGARD445.6 model surface grids: (a) structural (b) aerodynamic

2 Numerical methods

The following paragraphs summarize the overall methodology including the solution of the fluid-structure problem, the training and creation process of the reduced order models, for further information consult [7].

2.1 Fluid-structure interaction

For the solution of the coupled *fluid-structure interaction*(FSI) problem a partitioned implicit coupling scheme is applied to solve the Dirichlet-Neumann iteration. The data transfer and in-

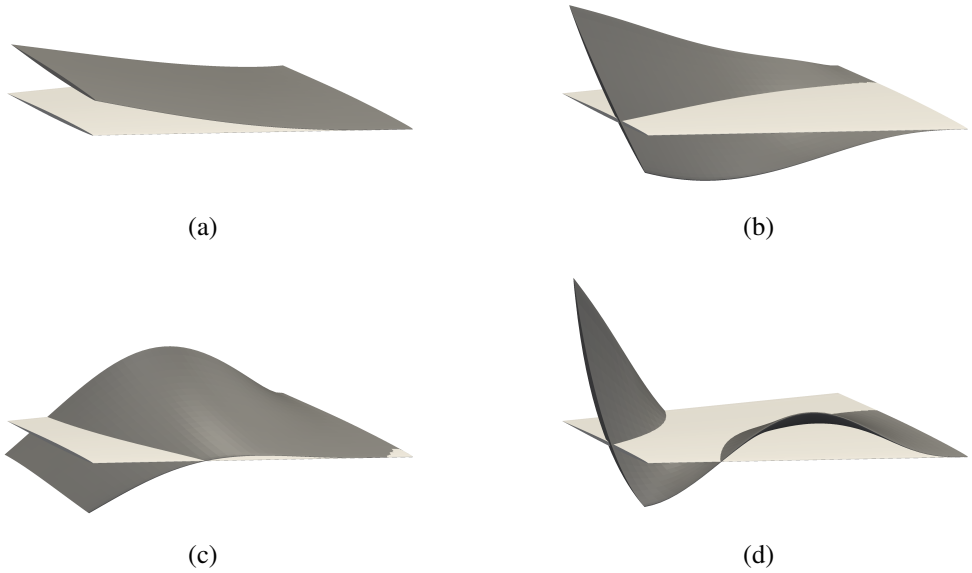

(a) (b)

(c) (d)

Figure 2: First four eigenmodes of the AGARD445.6-wing [7]: (a) first bending mode $\underline{\Phi}_1$; (b) first torsion mode $\underline{\Phi}_2$; (c) second bending mode $\underline{\Phi}_3$; (d) second torsion mode $\underline{\Phi}_4$

Mode	f_s/Hz	$f_{s,Unger}/Hz$	$f_{s,Yates}/Hz$
1	$9,813$	$9,813$	$9,60$
2	$38,795$	$38,800$	$38,10$
3	$50,514$	-	$50,70$
4	$94,119$	-	$98,50$

Table 1: Comparison of the eigenfrequencies of the employed structural mesh using the reference values from $f_{s,Unger}$ Unger [13] and the experimental detemined values of Yates [15]

terpolation of the displacements and forces between the nonconforming grids is established with *ifls*, see [5]. Using the *computational fluid mechanics*(CFD) solver TAU [11] for the solution of the Euler equation (Dirichlet boundary conditions) the unknown aerodynamic forces of the fluid surface mesh can be computed. The structural problem with Neumann boundary conditions is solved for the unknown structural displacements using a second order implicit newmark algorithm. The mass **M** and stiffness matrix **K** are exported from an ANSYS model.

CFD Gust calculation In contrast to a stochastic nature of atmospheric turbulence, a gust is considered in an idealized form as a discrete gust profile of disturbance velocities, see [14]. The CFD solver TAU provides a *disturbance velocity approach* (DVA) for the generation of discrete gust profiles. The DVA assumes that the disturbance velocities can be superimposed to the flow field by altering the flux balance, as described in [6], neglecting the mutual influence between the aircraft and the gust. One common gust profile for design purposes is the *1-cos* gust (see FAR25.341 [3]) where the disturbance velocities can be expressed as a function of time and

space

$$w_g(x_g) = \begin{cases} \frac{w_{g0}}{2}\left(1 - \cos\frac{2\pi x_g}{\lambda_g}\right) & 0 \leq x_g \leq \lambda_g \\ 0 & x_g < 0 \;||\; x_g > \lambda_g \end{cases} \tag{1}$$

with the gust wave length λ_g, the relative gust moving velocity U_g and the maximum disturbance velocity w_{g0}.

2.2 Training process

The training process consists of two steps and is summarized in the follwing paragraphs, for further information consult [7, 8, 9]:

1. Generation of training data by collecting forced displacements $u_f(t)$ and aerodynamic forces $F_f(t)$ using TAU

2. Model identification, construction of the ROM

In the first step the CFD data are calculated using an forced motion unsteady analysis in order to collect fluid displacements $\underline{u}_f(t)$ and corresponding force coefficients $\underline{c}_F(t) = \frac{\underline{F}_f(t)}{\frac{1}{2}\rho_\infty U_\infty^2 A_{ref}}$ values for each node of the aerodynamic surface mesh in every timestep t. The forced motion is defined by a superposition of the utilized modes in Eq. (2) and a sweep function in Eq. (3). The sweep function incorporates several features that can be tuned by parameters: The maximum amplitude of each mode is controlled by the maximum value of the generalised coordinate $q_{s,max}$, the exponential amplitude increase over time is controlled by k_{Amp} and the frequency modulation can be tuned with k_ω.

$$\underline{u}^f(t) = \sum_{s=1}^{3} q_s(t)\underline{\Phi}_s \tag{2}$$

$$q_s(t) = q_{s,max} \underbrace{(1 - e^{-k_{Amp}t})}_{\text{exp. amplitude increase}} \sin(\omega_s t(\underbrace{1 - 0,1\sin\left(\frac{\omega_s}{k_\omega}t\right)}_{\text{frequency modulation}})) \tag{3}$$

In the second step the ROM is build based on the training data. The elements of the ROM are depicted in Fig. 3:

Using the truncated *singular value decomposition*(SVD) as a *proper orthogonal decomposition*(POD) technique both the $\underline{u}_f(t)$ and $\underline{c}_F(t)$ can be mapped into an subspace and can be described with their corresponding POD coefficients $\underline{\hat{u}}_f(t)$, $\underline{\hat{c}}_f(t)$ (***input/ouput POD***, cp. Fig. 3). The mode truncation is established using a user-defined threshold value v_{red} and a partial sum criterion regarding the singular values σ_i of each mode, see e.g [12].

$$v = \frac{\sum_i^M \sigma_i}{\sum_j^q \sigma_j} \geq v_{red} \;\text{ mit }\; 0.0 \leq v_{red} \leq 1.0 \tag{4}$$

Combining a NARMA(*Nonlinear Autoregressive Moving Average*) ***Markov chain*** model [10] and a single layer RBF neuronal network[1] as the ***nonlinear mapping*** function $G(\underline{x})$, a surrogate function $\underline{\hat{c}}_F(t)$ can be defined Eq. (5). The surrogate function only depends on the

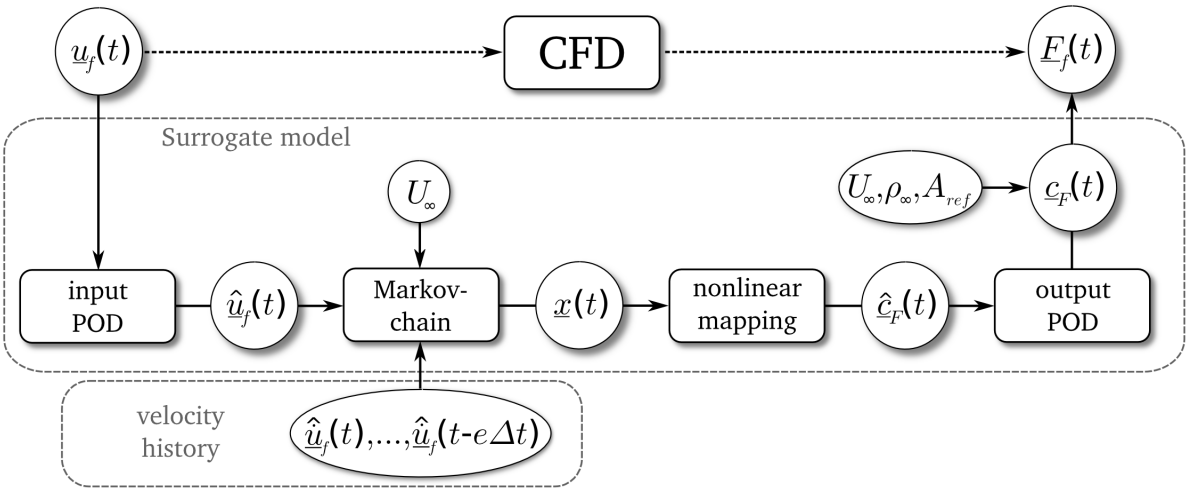

Figure 3: Modular process chain of the reduced order model

current static displacement input $\underline{\hat{u}}_f(t)$ and some discrete values for time history of unsteady velocities $\underline{\hat{\dot{u}}}_f$.

$$\underline{\hat{c}}_F(t) = G\left(\underbrace{\underline{\hat{u}}_f(t)}_{\text{steady part}}, \underbrace{\frac{\underline{\hat{\dot{u}}}_f(t)}{U_\infty}, \frac{\underline{\hat{\dot{u}}}_f(t - f_{sp}\Delta t)}{U_\infty}, \frac{\underline{\hat{\dot{u}}}_f(t - 2f_{sp}\Delta t)}{U_\infty}, \ldots, \frac{\underline{\hat{\dot{u}}}_f(t - l_{\dot{u}}\Delta t)}{U_\infty}}_{\text{unsteady part}}\right) \tag{5}$$

where $f_{sp} \in \mathbb{N}$ is defined as a sparse factor that reduces the number of input parameters by considering only each f_{sp}th time step in the history of velocities.
For all simulations a time window number of $l_{\dot{u}} = 50$, an unsteady physical time step size of $\Delta t = 0.001$ and a sparse factor of $f_{sp} = 5$ are employed.

Handling of gusts in ROM approach The main idea for the incorporation gust disturbance velocities - as published in [7] - is to superimpose the disturbance velocities $\underline{w}_g(t)$ with the structural displacements velocities $\underline{\dot{u}}_f(t)$ to form a modified velocity distribution $\underline{\dot{u}}_{f+g}(t) = \underline{\dot{u}}_f(t) + \underline{w}_g(t)$. Consequently the surrogate function Eq. (5) is modified to

$$\underline{\hat{c}}_F(t) = G\left(\underline{\hat{u}}_f(t), \frac{\underline{\hat{\dot{u}}}_{f+g}(t)}{U_\infty}, \frac{\underline{\hat{\dot{u}}}_{f+g}(t - f_{sp}\Delta t)}{U_\infty}, \ldots, \frac{\underline{\hat{\dot{u}}}_{f+g}(t - l_{\dot{u}}\Delta t)}{U_\infty}\right) \tag{6}$$

2.2.1 Elastic modes trained ROM E

In the training data generation step only the first three elastic eigenmodes (Table 1) of the AGARD wing are choosen in the forced motion process using Eq. (2). Two analyses with the maximum values of the generalized coordinates as listed in Table 2 are performed and the resulting matrices $\underline{u}_{f,E}(t)$ and $\underline{c}_{F,E}(t)$ serve as input for the training process.

Under the flow conditions listed in Table 3, 1000 time steps are calculated using empirical parameters of $k_{Amp} = 5$ and $k_\omega = 25$, compare Eq. (3).

Analyse	$q_{1,max}$	$q_{2,max}$	$q_{3,max}$
I	0.02	0.005	0.004
II	0.04	0.01	0.008

Table 2: Maximum values of the generalized coordinates of the forced motion analysis

parameter	value	parameter	value
Ma	$0,901$	ρ_∞	$1,29251\ \frac{kg}{m^3}$
p_∞	$101325,0\ Pa$	U_∞	$298,49\ \frac{m}{s}$
T_∞	$273,15\ K$	α	$0°$

Table 3: Flow conditions

Using the truncation criterion of Eq. (4) with $v_{red} = 0.99$ results in 3 input POD modes (accoring to the three exited eigenmodes) and 254 output POD modes.

2.2.2 Gust trained ROM G

In order to generate a gust training set a gust analysis over the rigid wing is performed using the already mentioned flow conditions (Table 3) and the following gust parameters:

The relative gust moving velocity u_g is set to U_∞ and the gust wave length λ_g is calculated as follows in order to exite the first structural eigenmode $f_{s,1}$.

$$\lambda_g = \frac{U_{\text{inf}}}{f_{s,1}} = 30.4179m \tag{7}$$

In every timestep the disturbance velocities $\underline{w}_g(t)$ as well as the force coefficients $\underline{c}_{F,G}(t)$ are collected from three analyses with varying maximum disturbance velocities, see Table 4.

Gust analysis	w_{g0}
I	$4\ \frac{m}{s}$
II	$8\ \frac{m}{s}$
III	$20\ \frac{m}{s}$

Table 4: maximum gust disturbance velocities for all three gust analyses for the rigid wing

For the ROM identification process virtual deformations $\underline{u}_{f,G}(t) = \underline{w}_g(t) \cdot \Delta t$ are calculated and serve as the only input for the ROM training process. The reduced order model G is thus trained with $\underline{u}_f(t) = \underline{u}_{f,G}(t)$ and $\underline{c}_F(t) = \underline{c}_{F,G}(t)$ of all three gust analyses. Consequently using Eq. (4) with a reduction threshold value of $v_{red} = 0.999$ overall 2 input modes and 21 output modes are identified.

2.2.3 Gust trained ROM GE

For the reduced order model GE that should predict the elastic as well as the gust CFD response no new data has to be generated. It is trained with forced motion data of 2.2.1 and 2.2.2 and thus with $u_f(t) = \underline{u}_{f,E}(t) \cup \underline{u}_{f,G}(t)$ and $c_f(t) = \underline{c}_{F,E}(t) \cup \underline{c}_{F,G}(t)$. Consequently using Eq. (4) with a reduction threshold value of $v_{red} = 0.999$ overall 4 input POD modes and 246

output POD modes are identified which means that one additional input POD mode is identified compared to ROM E.

3 Results

In the following section the results for the CFD and ROM calculation are compared. In the first sections the results for a gust over the rigid AGARD wing are compared for the flow conditions depicted in Table 3. Finally the gust trained ROMs are employed in an aerostructural coupling environment.

3.1 Rigid - ROM E

Fig. 4 shows the comparative results for the rigid setup, i.e. no deformations of the strucutural model are considered. The reduced order model E can predict the the time response accurately but the amplitude of the gust is underestimated, due to the improper training set. The exited strutural modes in the training set do not include displacements at the wing root and thus disturbance velocities in the root of the wing cannot be taken into account, as alreay argued in [7]. Thus an improved training set should at least include modes with displacements/velocities at the wing root.

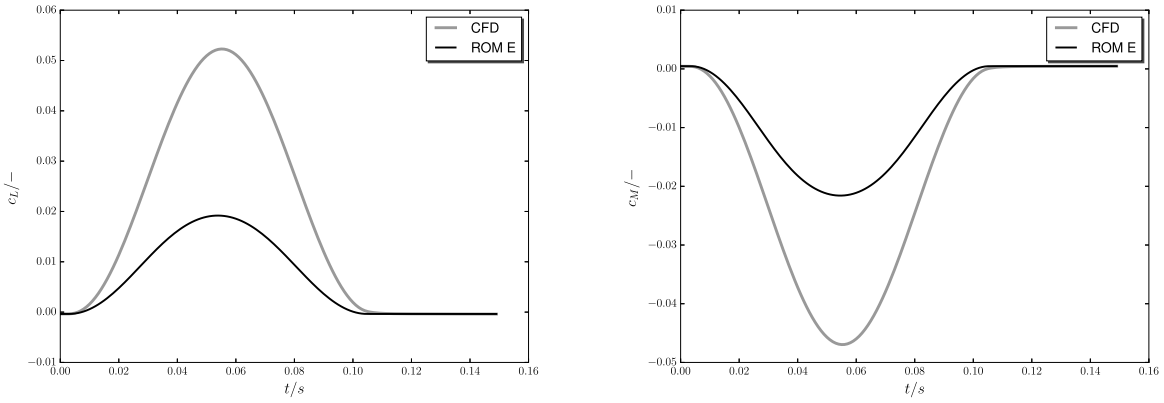

(a) (b)

Figure 4: CFD versus ROM E results: (a) global lift coefficient c_L (b) global moment coefficient c_M

3.2 Rigid - gust trained ROMs

Comparing the global lift c_L and moment c_M coefficient both the gust trained models can predict the gust response of the CFD analysis for the rigid setup, see Fig. 5.

3.3 CFD-CSM and ROM-CSM coupling results

In Fig. 6 the results for the aeroelastic AGARD wing being exposed to a *1-cos* gust with a maximum disturbance velocity of $w_{g0} = 2\frac{m}{s}$ are depicted. Due to the zero angle of attack the wing is initially in rest and reacts to the gust induced change in angle of attack with an increase in lift and hence it deflects. After the gust has completly passed the wing at $t = 0.107$ the wing exibits flutter, as reported by [15] for these flow conditions (see Table 3).
As expected the ROM G - only trained with pseudo disturbance velocities - isn't capable of predicting the aerodynamic response of the elastically deforming wing.

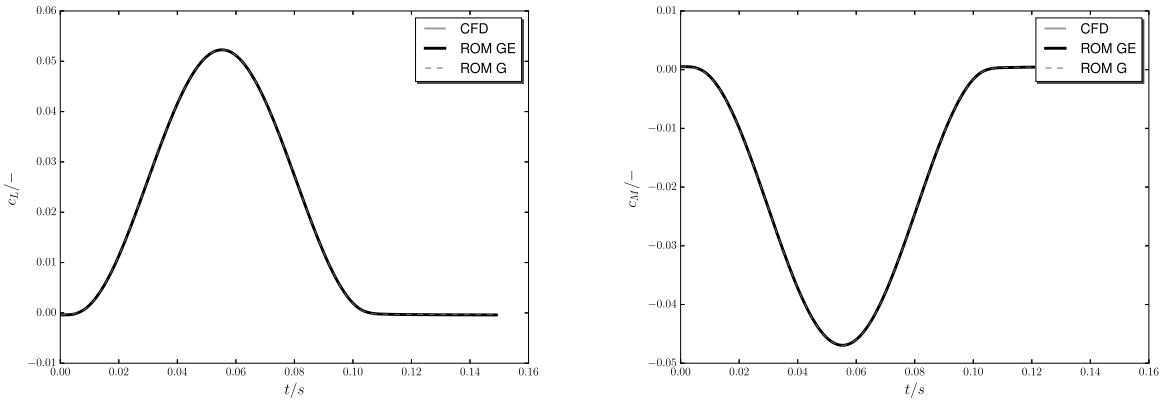

(a) (b)

Figure 5: Results for ROM G and GE compared to CFD: (a) global lift coefficient c_L (b) global moment coefficient c_M

The ROM GE - incorporation both gust and elastic modes - can predict the reaction of the wing quite well showing only slight deviations in c_L and $u_{z,Tip}$. The maximum disturbance velocity is limited here to $w_{g0} = 2\frac{m}{s}$ because at higher values the maximum displacement would exceed the maximum trained value, see Table 2. In order to capture higher disturbance velocities the training with elastic modes should be set up with increased maximum generalised coordinates $q_{i,max}$.

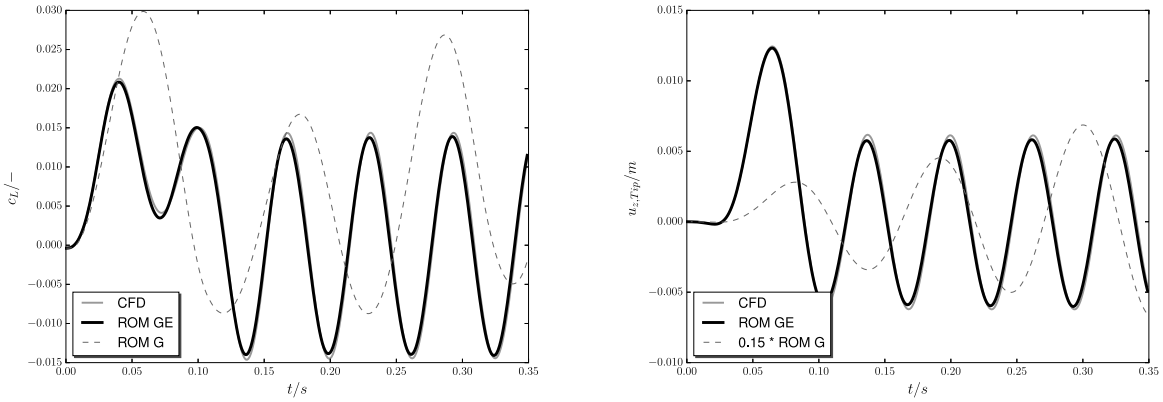

(a) (b)

Figure 6: FSI results for model GE with gust amplitude $w_{g0} = 2\frac{m}{s}$: (a) global lift coefficient c_L (b) structural displacement of tip node $u_{z,Tip}$

4 CONCLUSIONS

Three different reduced order models have been compared for a gust over a rigid AGARD model. The first ROM trained only with the structural elastic eigenmodes cannot sufficiently capture the gust response, due to missing training modes including displacements and velocities at the wing root.

Both gust trained models without elastic modes (ROM G) and including elastic modes (ROM GE) can accurately predict the gust response in the rigid setup.

In the FSI simulation only the gust *and* elastic modes trained ROM GE can successfully predict the aerostructural behaviour of the AGARD wing in the transonic flight regime. In addition the enhanced ROM GE can still be used to predict the flutter boundary and thus can serves as a surrogate model for multiple flow conditions.

Future studies should include parameter variations for different gust shapes and amplitudes. In addition the presented method could be applied to different configurations, e.g. more realistic 3D configurations including viscous effects. It could also be coupled with flight mechanical simulations in order to resolve the dynamic response of the aircraft.

REFERENCES

[1] D. S. Broomhead and D. Lowe. Multivariable functional interpolation and adaptive networks. *Complex Systems*, 2:321–355, 1988.

[2] D. Dimitrov and R. Thormann. DLM-correction method for aerodynamic gust response prediction. *Proceedings" IFASD 2013"*, 2013.

[3] F.A.A. FAR 25.341 Online Document, Feb. 2016.

[4] H. Haddad Khodaparast, G. Georgiou, J. Cooper, L. Riccobene, S. Ricci, G. Vio, and P. Denner. Efficent worst case"1-cosine" gust loads prediction. *Journal of Aeroelasticity and Structural Dynamics*, 2(3), 2012.

[5] M. Haupt, R. Niesner, R. Unger, and P. Horst. Computational Aero-Structural Coupling for Hypersonic Applications. In *9th AIAA/ASME Joint Thermophysics and Heat Transfer Conference*, 2006. San Francisco, California, USA.

[6] R. Heinrich and L. Reimer. Comparison of different approaches for gust modeling in the CFD Code TAU. In *International Forum on Aeroelasticity and Structure Dynamics, Bristol*, 2013.

[7] K. Lindhorst. *Nichtlineare Ersatzmodellierung in transsonischer instationärer Aeroelastik*. PhD thesis, 2015. Forschungsbericht 2015-01.

[8] K. Lindhorst, M. Haupt, and P. Horst. Efficient surrogate modelling of nonlinear aerodynamics in aerostructural coupling schemes. *AIAA Journal*, 52(9):1952–1966, 2014.

[9] K. Lindhorst, M. Haupt, and P. Horst. Aeroelastic Analyses of the High-Reynolds-Number-Aerostructural-Dynamics Configuration Using a Nonlinear Surrogate Model Approach. *AIAA Journal*, 53(9):2784–2796, 2015.

[10] S. P. Meyn and R. L. Tweedie. *Markov chains and stochastic stability*. Springer London Ltd., London, 1993.

[11] D. Schwamborn, T. Gerhold, and V. Hannemann. On the Validation of the DLR-TAU Code. In *New Results in Numerical and Experimental Fluid Mechanics II*, pages 426–433. Springer, 1999.

[12] H. Spiess. *Reduction methods in finite element analysis of nonlinear structural dynamics*. PhD thesis, 2006.

[13] R. Unger, M. C. Haupt, and P. Horst. Coupling techniques for computational non-linear transient aeroelasticity. *Proceedings of the Institution of Mechanical Engineers, Part G: Journal of Aerospace Engineering*, 222(4):435–447, 2008.

[14] J. R. Wright and J. E. Cooper. *Introduction to aircraft aeroelasticity and loads*. John Wiley & Sons, Ltd., 2007.

[15] E. C. Yates. AGARD standard aeroelastic configuration for dynamic response, candidate configuration I. *Wing 445.6, NASA TM-100462, Langley Research Center, Hampton, VA*, 1987.

[16] W. Zhang, B. Wang, Z. Ye, and J. Quan. Efficient method for limit cycle flutter analysis based on nonlinear aerodynamic reduced-order models. *AIAA journal*, 50(5):1019–1028, 2012.

[17] W. Zhang, Z. Ye, Q. Yang, and A. Shi. Gust response analysis using CFD-based reduced order models. In *47th AIAA Aerospace Sciences Meeting Including The New Horizons Forum and Aerospace Exposition, AIAA Paper*, volume 895, 2009.